Original Article

Magnetic resonance image compilation sequence to quantitatively detect active sacroiliitis with axial spondyloarthritis

Yunping Jiang[1,2#], Wenjuan Li[1#], Jing Zheng[3], Ke Zhang[1], Chaoran Liu[1], Guobin Hong[1]^

[1]Department of Radiology, the Fifth Affiliated Hospital, Sun Yat-sen University, Zhuhai, China; [2]Department of Radiology, the First Affiliated Hospital, Zhejiang University School of Medicine, Hangzhou, China; [3]Department of Rheumatology and Immunology, the Fifth Affiliated Hospital, Sun Yat-sen University, Zhuhai, China

Contributions: (I) Conception and design: Y Jiang, W Li, G Hong; (II) Administrative support: G Hong; (III) Provision of study materials or patients: Y Jiang, J Zheng, G Hong; (IV) Collection and assembly of data: Y Jiang, K Zhang, C Liu; (V) Data analysis and interpretation: Y Jiang, W Li; (VI) Manuscript writing: All authors; (VII) Final approval of manuscript: All authors.

[#]These authors contributed equally to this work.

Correspondence to: Guobin Hong. Department of Radiology, the Fifth Affiliated Hospital, Sun Yat-sen University, Zhuhai 519000, China. Email: honggb@mail.sysu.edu.cn.

Background: To evaluate the diagnostic value of quantitative parameters [T1, T2, and proton density (PD) value] generated from magnetic resonance image compilation (MAGiC) sequence for active sacroiliitis in the patients with axial spondyloarthritis (ax-SpA).

Methods: A total of 90 consecutive ax-SpA patients were recruited and divided into an active group (n=48) and inactive group (n=42) based on the Spondyloarthritis Research Consortium Canada (SPARCC) score in this prospective study. In addition, 47 healthy volunteers were recruited as the control group. All participants underwent magnetic resonance (MR) scanning (including MAGiC sequence and T2 mapping sequence) to obtain the T1 value, T2 value, PD value of MAGiC sequence (MAGiC T1 value, T2 value, PD value), and the T2 value of T2 mapping sequence (T2 map T2 value). Intraclass correlation coefficients (ICC) were calculated to assess the inter- and intra-observer agreement. The correlation between the MAGiC T2 value and the T2 map T2 value was analyzed using Spearman's Rho. One-way analysis of variance (ANOVA) and receiver operating characteristic (ROC) analysis were performed for all parameters.

Results: For the active group, inactive group, and control group, the MAGiC T1 value, T2 value, PD value, and T2 map T2 value were (1,700.91±725.40, 546.58±59.49, 640.25±95.79 ms), (129.37±23.85, 117.16±20.37, 90.52±12.05 ms), (76.47±15.92, 82.69±9.51, 75.51±9.17 pu), and (96.75±16.06, 87.96±9.27, 82.03±10.17 ms), respectively. The difference of the MAGiC T1 value and the MAGiC T2 value in the three groups was statistically significant (P<0.05). The MAGiC PD value was only statistically significant between inactive and control groups (P=0.001). When comparing the ROC curves of quantitative values among the three groups, MAGiC T1 value showed higher diagnostic efficacy than MAGiC T2 value between the active and inactive groups (MAGiC $T1_{AUC}$: 0.971, MAGiC $T2_{AUC}$: 0.655, P<0.0001), and the MAGiC T2 value showed higher diagnostic efficacy than T2 map T2 value between the active group and control group, and the inactive group and control group (MAGiC $T2_{AUC}$: 0.940, T2 map $T2_{AUC}$: 0.784, P=0.0021; MAGiC $T2_{AUC}$: 0.877, T2 map $T2_{AUC}$: 0.644, P=0.0011). The consistency of measurements was excellent (ICC =0.972–0.998). The MAGiC T2 value was positively correlated with the T2 map T2 value, but with a low correlation (r=0.402; P<0.001).

Conclusions: A significant difference was detected between the MAGiC T1 and T2 values among

^ ORCID: 0000-0002-2690-7802.

the three groups, while MAGiC PD value had limited diagnostic value. MAGiC T1 value was better at differentiating the active group and inactive group than MAGiC T2 value. MAGiC T2 value was better at differentiating the active group and control group, the inactive group and control group than T2 map T2 value.

Keywords: Sacroiliitis; axial spondyloarthritis (ax-SpA); magnetic resonance imaging (MRI); MAGiC sequence; quantitative analysis

Submitted Oct 02, 2021. Accepted for publication Apr 12, 2022.
doi: 10.21037/qims-21-972
View this article at: https://dx.doi.org/10.21037/qims-21-972

Introduction

Axial spondyloarthritis (ax-SpA) is a group of chronic inflammatory diseases that mainly affects the sacroiliac joints (SIJ). Misdiagnosis or delayed diagnosis can result in missing the best time for treatment, leading to aggravation of the condition and even disability (1). Sacroiliitis is a key point for diagnosing and treating ax-SpA; bone marrow edema (BME) is the essential active index for diagnosing sacroiliitis in ax-SpA patients (2). Magnetic resonance imaging (MRI) is now a preferred imaging method to detect BME in sacroiliitis as it is non-invasive, has high soft-tissue resolution and multi-parameter and multi-directional imaging, and does not involve ionizing radiation (3,4). However, the conventional T2-weighted sequence with fat suppression (T2WI FS) is limited to qualitative evaluation and does not provide quantitative information.

In recent years, using quantitative or semi-quantitative MRI methods has gained much attention. Dynamic contrast-enhanced MRI can generate semi-quantitative hemodynamic parameters to assess the activity of sacroiliitis in patients with ankylosing spondyloarthritis (AS) and evaluate the curative effect of treatment (5). However, injection of the MRI contrast agent is costly and may increase the risk of renal fibrosis (6). Diffusion-weighted imaging (DWI) can quantify the degree of sacroiliitis inflammatory lesions without relying on contrast agents because it uses the value of the apparent diffusion coefficient (ADC) found by measuring the random movement of water molecules (7); however, DWI lacks inter-observer consistency (8). Incoherent motion diffusion-weighted imaging (IVIM-DWI) can simultaneously obtain pure water molecular diffusion motion information and capillary perfusion information as a multi-b value DWI sequence with biexponential mode (9). Zhao *et al.* (10) reported that the pure diffusion coefficient (Dslow) can be used as an independent parameter to distinguish between active and inactive AS patients and can improve the sensitivity and specificity combined with the microvascular volume fraction (f). Nevertheless, the low image resolution of IVIM-DWI makes it challenging to accurately locate the lesions in a capacity similar to that of DWI. Furthermore, the T2 mapping sequence is a multi-echo pulse sequence that can be used to evaluate the cartilage and bone marrow lesions of the SIJ by detecting changes in water molecules, collagen content, and tissue anisotropy, but its values are easily affected by surrounding tissues (11-13).

Magnetic resonance image compilation (MAGiC) sequence is one type of synthetic magnetic resonance imaging (SyMRI) that can obtain multiple contrast-weighted imaging and multiple sets of quantitative images in one acquisition (14). MAGiC can provide a qualitative diagnosis and generate multiple quantitative maps to provide direct values of lesions. According to recent studies, although this technology continues to be applied to musculoskeletal imaging (15-18), there are no related clinical applications of the MAGiC sequence to SIJ diseases.

Therefore, we aimed to evaluate the diagnostic value of MAGiC quantitative parameters [MAGiC T1 value, T2 value, and proton density (PD) value] for active sacroiliitis in ax-SpA patients and a heathy control group, and explore the correlation between the T2 value of MAGiC sequence and T2 mapping sequence. We present the following article in accordance with the STARD reporting checklist (available at https://qims.amegroups.com/article/view/10.21037/qims-21-972/rc).

Methods

Participants

The study was conducted in accordance with the

Table 1 Acquisition parameters of MRI

Variables	T1WI	T1WI	T2WI FS	T2WI FS	T2 mapping	MAGiC
Orientation	OAx	Ocor	OAx	Ocor	Ocor	Ocor
TR (ms)	551	734	2,285	3,191	1,348	4,000
TE (ms)	Min full	Min full	68	68	6.9	Auto
FOV (mm^2)	240×240	240×240	240×240	240×240	240×240	240×240
Matrix	320×256	320×256	320×256	320×256	320×256	320×256
Thickness/gap (mm)	4/1	4/1	4/1	4/1	4/1	4/1
Echo train length, n	3	3	15	16	–	16
NEX	2	2	4	4	1	1
Scanning time	1 min 24 s	2 min 12 s	2 min 29 s	3 min 02 s	8 min 41 s	6 min 08 s

MRI, magnetic resonance imaging; T1WI, T1 weighted imaging; T2WI FS, fat-suppressed T2-weighted imaging; MAGiC, magnetic resonance image compilation; OAx, oblique axial; Ocor, oblique coronal; TR, repetition time; TE, echo time; FOV, field of view; NEX, number of excitation.

Declaration of Helsinki (as revised in 2013). The study was approved by Ethics Committee of the Fifth Affiliated Hospital of Sun Yat-sen University [No. K160-1(2019)], and informed consent was provided by all individual participants. A total of 90 patients who met the latest diagnostic criteria for ax-SpA (19) as diagnosed by rheumatologists were included consecutively in this study from November 2019 to January 2021 and underwent MRI examinations. We excluded patients with MRI examination contraindications, with a history of other types of spondyloarthritis or relevant dysplasia, trauma, surgical marks, severe infection, tumors, or other diseases found in the SIJ, and those with incomplete examinations or examinations with artifacts. A total of 47 healthy volunteers older than 18 years (28 men, 19 women; mean age: 26.0±6.6 years) were recruited as the control group; those found to have SIJ lesions were excluded.

MR protocol

All participants underwent SIJ MR examinations on a 3.0 T scanner (Signa Pioneer, GE Healthcare, Milwaukee, WI, USA) using a body coil and 16-channel abdomen phased-array coil. The MRI included conventional SIJ sequences, the T2 mapping sequence, and the MAGiC sequence. More detailed acquisition parameters are shown in *Table 1*.

Image analysis

Spondyloarthritis Research Consortium Canada (SPARCC) score

According to the SPARCC score (20), two radiologists [radiologist 1 (10 years of work experience), radiologist 2 (8 years of work experience)] engaged in musculoskeletal system imaging and scored the images in the T2WI FS sequence together combined with clinical information. In the case of disagreement, a consensus was sought for the final decision. SPARCC score ≥2 was classified as the active sacroiliitis group (active group), while SPARCC score <2 was classified as the inactive sacroiliitis group (inactive group) (11). The Assessment of SpondyloArthritis international Society (ASAS) definition of BME was a high signal on the T2WI FS sequence or Short Tau Inversion Recovery (STIR) sequence and a low signal on the T1WI sequence (using sacral intervertebral foramina bone marrow signal as reference) in subchondral bone shown in the MRI. Definite BME was required to be displayed on more than 2 levels (sequence or orientation) or multiple lesions in one level for accurately scoring (21).

Image processing and measurements

The T2 mapping sequence and MAGiC sequence images were processed by the GE AW4.7 workstation function

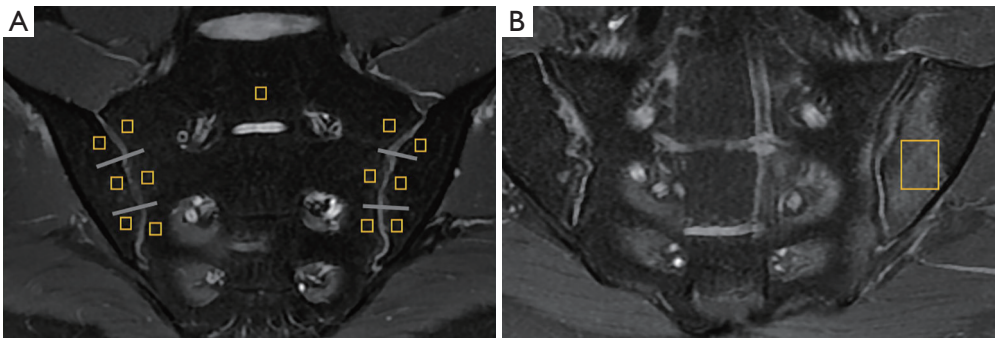

Figure 1 Schematic diagram of ROI placement for SIJ. (A) For the inactive group and the control group, the ROI (yellow frame) was placed on each side of the SIJ (six regions, separated by white line) on a slice displaying the most complete sacroiliac articular cartilage. (B) For the active group, the ROI (yellow frame) was placed in the center of the BME in as large an area as possible. ROI, area of interest; SIJ, sacroiliac joint; BME, bone marrow edema.

tool model (GE Healthcare) and the MR scanner console MAGiC model.

Two radiologists [radiologist 3 (6 years of work experience), radiologist 4 (3 years of work experience)] engaged in musculoskeletal system imaging independently placed the region of interest (ROI) in a double-blind manner with reference to the T2WI FS sequence.

The overall measurement principles were established as follows: for the active group, the ROI was manually placed in the center of the BME and was made as large as possible. The average values of multiple lesions measured were used as the final values. For inactive group and control group, the ROI was manually placed on each side of the SIJ (six regions) on a slice displaying the most complete sacroiliac articular cartilage, and the average values of ROIs measured were used as the final values (*Figure 1*). Artifacts, SIJ bone cortex, sclerosis, blood vessels, and the cystic area were avoided while placing the ROI. Finally, we obtained the T2 map T2 value, the MAGiC T1 value, the MAGiC T2 value, and the MAGiC PD value. Two weeks later, radiologist 3 measured all parameters again.

Statistical analysis

All data analysis was performed using SPSS 25.0 (IBM Corp., Armonk, NY, USA), GraphPad Prism 8 (GraphPad Software, San Diego, CA, USA), and MedCalc (MedCalc Software, Ostend, Belgium) statistical software. A P value <0.05 indicated a statistically significant difference.

The differences of basic clinical data and quantitative values among the three groups were compared by one-way analysis of variance (ANOVA). The inter- and intra-observer consistency were determined by the intraclass correlation coefficient (ICC) (ICC <0.40, poor; ICC =0.40–0.59, fair; ICC =0.60–0.74, good; ICC ≥0.75, excellent). The correlation between the MAGiC T2 value and the T2 map T2 value was graded by Spearman's Rho (r=0, no correlation; |r| <0.3, weak correlation; |r| =0.3–0.5, low correlation; |r| =0.5–0.8, significant correlation; |r| >0.8, high correlation; |r| =1, complete correlation). Receiver operating characteristic (ROC) curves were used to analyze the diagnostic efficacy of quantitative values among the three groups.

Results

Clinical characteristics of ax-SpA patients

A total of 90 ax-SpA patients were included in this study (*Figure 2*). *Table 2* shows that there were no significant differences in gender, age, height, weight, and body mass index (BMI) between the active group and the inactive group (P>0.05), but there was a significant difference in the symptom of lower back pain between the two groups (P<0.05). There were no adverse events reported due to conduction of the MAGiC sequence.

Analysis results of inter- and intra-observer consistency

A total of 137 participants were included in this study (95 men, 42 women; mean age: 30.3±8.4 years). Inter- and intra-observer consistency of quantitative values were all good (ICC =0.972–0.998; *Table 3*).

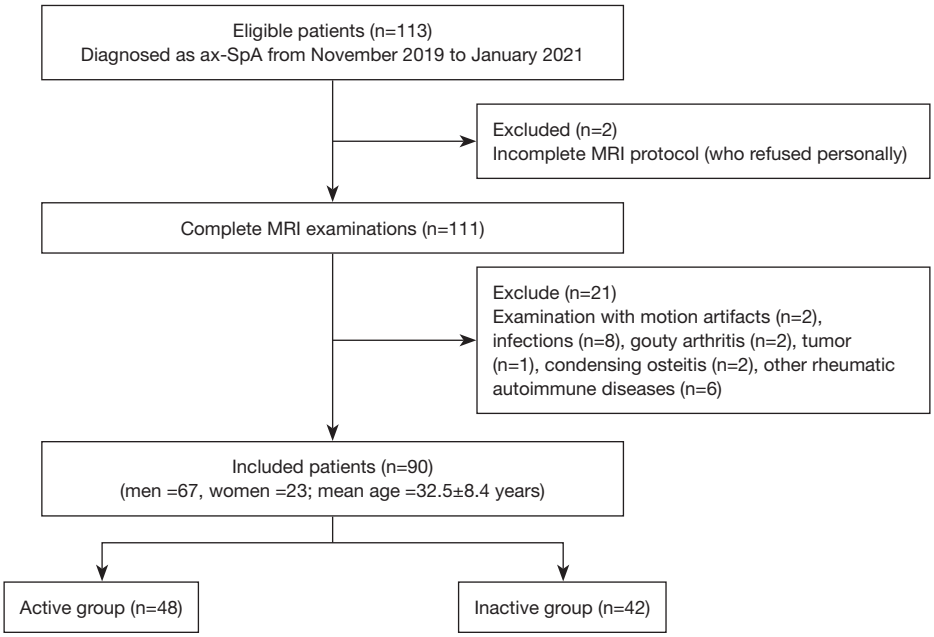

Figure 2 Flow diagram of the study participants. ax-SpA, axial spondyloarthritis; MRI, magnetic resonance imaging.

Table 2 Clinical characteristics of ax-SpA patients

Characteristic	Active group (n=48)	Inactive group (n=42)	P value
Gender	14 (F)/34 (M)	9 (F)/33 (M)	0.680
Age (years)	30.79±7.60	34.50±8.89	0.094
Height (m)	1.67±0.08	1.70±0.08	0.270
Weight (kg)	62.48±11.97	65.77±10.47	0.349
BMI (kg/m^2)	22.21±3.42	22.72±3.10	0.741
Lower back pain	40 (Y)/8 (N)	26 (Y)/16 (N)	<0.05

ax-SpA, axial spondyloarthritis; F, female; M, male; BMI, body mass index; Y, yes; N, no.

Table 3 Inter- and intra-observer agreement of MAGiC sequence and T2 mapping sequence

Variables	Intra-reader agreement	Inter-reader agreement
MAGiC T1 value	0.996 (0.995, 0.997)	0.996 (0.995, 0.997)
MAGiC T2 value	0.985 (0.979, 0.989)	0.986 (0.980, 0.990)
MAGiC PD value	0.979 (0.970, 0.985)	0.972 (0.959, 0.980)
T2 map T2 value	0.992 (0.988, 0.994)	0.990 (0.986, 0.993)
Total	0.998 (0.998, 0.999)	0.998 (0.998, 0.999)

95% confidence interval for difference in parentheses. MAGiC, magnetic resonance image compilation; PD, proton density.

Table 4 Test of MAGiC and T2 mapping parameters among the three groups by ANOVA

Variables	Active group	Inactive group	Control group	P value
MAGiC T1 value (ms)	1,700.91±725.40	546.58±59.49	640.25±95.79	<0.001#^*
MAGiC T2 value (ms)	129.37±23.85	117.16±20.37	90.52±12.05	<0.001#*; 0.028^
MAGiC PD value (pu)	76.47±15.92	82.69±9.51	75.51±9.17	0.001#
T2 map T2 value (ms)	96.75±16.06	87.96±9.27	82.03±10.17	0.003^; <0.001*

#, inactive group *vs*. control group; ^, active group *vs.* inactive group; *, active group *vs.* control group. MAGiC, magnetic resonance image compilation; ANOVA, analysis of variance; PD, proton density.

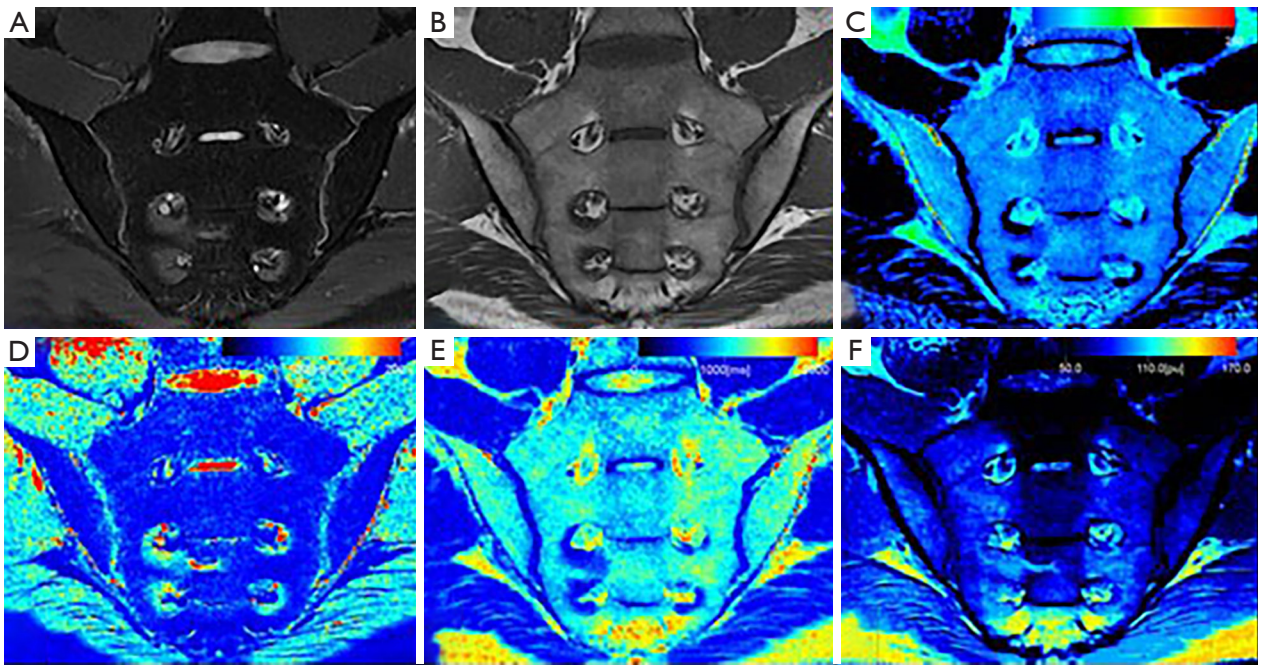

Figure 3 Example cases. Images of a 27-year-old healthy man with normal SIJ. The bilateral SIJ surfaces are smooth. T2WI FS sequence (A), T1WI sequence (B) show no abnormal signal; T2 mapping sequence (C), MAGiC T1 mapping sequence (D), MAGiC T2 mapping sequence (E), and MAGiC PD mapping sequence (F) show no abnormal pseudo-color display. SIJ, sacroiliac joint; T2WI FS, fat-suppressed T2 weighted imaging; T1WI, T1 weighted imaging; MAGiC, magnetic resonance image compilation; PD, proton density.

Measurement results of MAGiC sequence and T2 mapping sequence

Table 4 shows the specific quantitative values of each group. The MAGiC T1 value, MAGiC T2 value, and T2 map T2 value of the active group were all higher than those of the inactive and control groups, and these quantitative values of the inactive group were higher than those of the control group. The differences of the MAGiC T1 value and the MAGiC T2 value in the three groups were statistically significant (P<0.05). The differences of the T2 map T2 value between the active group and the inactive group, and between the active group and the control group, were statistically significant (P<0.05). The MAGiC PD value was only statistically significant between the inactive and control groups (P=0.001). *Figures 3-5* shows MR images of normal SIJ, active sacroiliitis, and inactive sacroiliitis.

ROC curves analysis

The ROC curve analyses of quantitative values for the three groups are shown in *Figure 6* and *Table 5*.

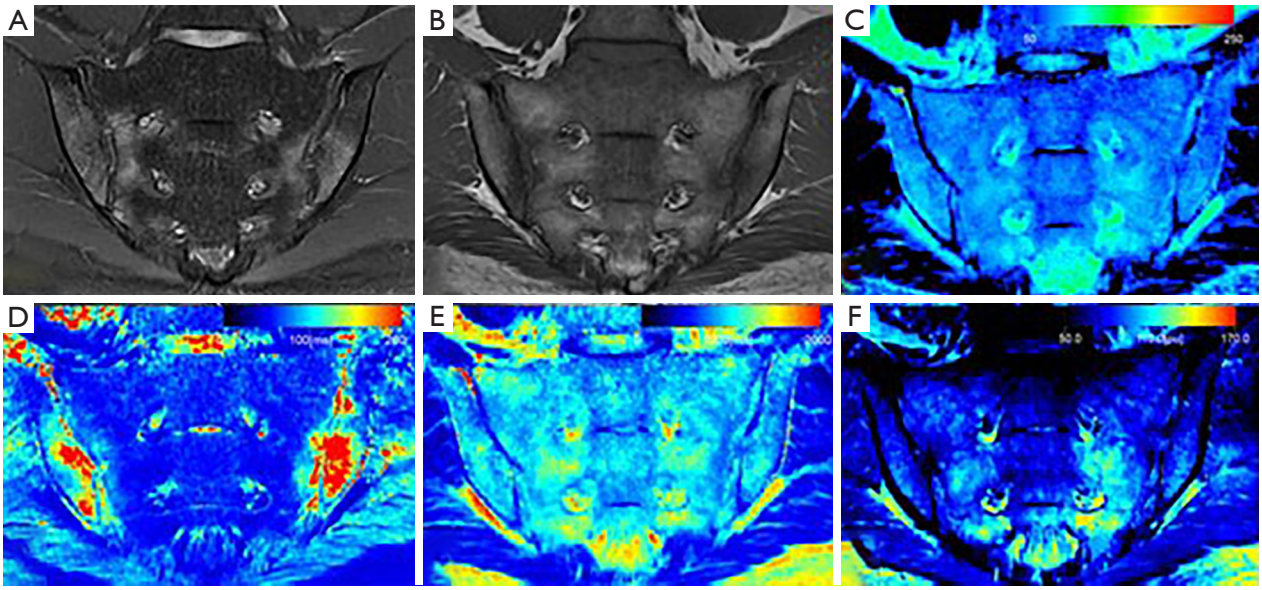

Figure 4 Example cases. Images in a 26-year-old man with active sacroiliitis of ankylosing spondylitis. The bilateral SIJ surfaces are rough with focal bone erosions. T2WI FS sequence (A) and T1WI sequence (B) show BME in the subchondral bone marrow. The corresponding areas display red or yellow-green in MAGiC T1 mapping sequence (D) and yellow-green in the MAGiC T2 mapping sequence (C). T2 mapping sequence (E) and the MAGiC PD mapping sequence (F) show no abnormal pseudo-color display. SIJ, sacroiliac joint; T2WI FS, fat-suppressed T2 weighted imaging; T1WI, T1 weighted imaging; BME, bone marrow edema; MAGiC, magnetic resonance image compilation; PD, proton density.

The MAGiC T1 value showed higher diagnostic efficacy than the MAGiC T2 value between the active and inactive groups (P<0.0001). The MAGiC T1 value showed higher diagnostic efficacy than T2 map T2 value between active and inactive groups, active and control groups, inactive and control groups (P<0.0001, P=0.0054, and P=0.0106, respectively). There was no significant difference in the diagnostic efficiency of the MAGiC T1 value and MAGiC T2 value between the active group and the control group, and between the inactive group and the control group (P=0.9724 and P=0.1254, respectively).

The MAGiC T2 value showed higher diagnostic efficacy than the T2 map T2 value between the active and control groups, and between the inactive and control groups (P=0.0021 and P=0.0011, respectively). There was no significant difference in the diagnostic efficiency of the MAGiC T2 value and the T2 map T2 value between the active group and inactive group (P=0.7017).

Correlation analysis of T2 value between MAGiC sequence and conventional T2 mapping sequence

The MAGiC T2 value was positively correlated with the T2 map T2 value, with low correlation (r=0.402; P<0.001; *Figure* 7).

Discussion

The MAGiC sequence is a new MRI quantitative technology. Rather than conventional MRI sequence, MAGiC sequence offers multiple additional quantitative images and obtains arbitrary contrast images by adjusting the echo time (TE), repetition time (TR), and reversal time to meet different demands for clinical diagnosis (14). The MAGiC sequence requires a shorter time and is highly efficient, making it more suitable for ax-SpA patients who frequently experience aggravation of lower back pain at rest. In addition, the reconstructed images of the MAGiC sequence show the same layer, which helps localize and compare lesions.

Our results showed that both the MAGiC T1 value and MAGiC T2 value have diagnostic value for detecting active sacroiliitis in ax-SpA patients, and the performance of the MAGiC T1 value was better than MAGiC T2 value with higher sensitivity and specificity. The T2 value is sensitive to the slow molecular motion of water protons

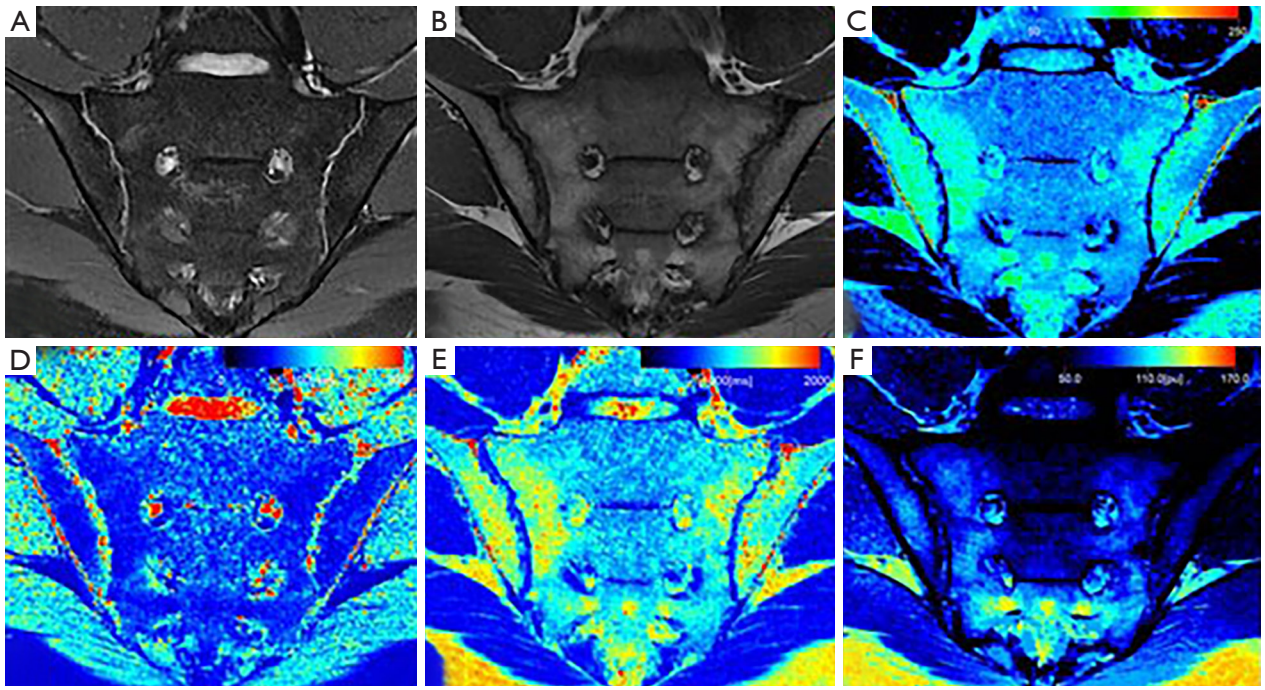

Figure 5 Example cases. Images in a 20-year-old man with inactive sacroiliitis of ankylosing spondylitis. The bilateral SIJ surfaces are rough with focal bone erosions. T2WI FS sequence (A) and T1WI sequence (B) show no BME existing. However, subchondral bone marrow displays yellow-green with mottled red in the MAGiC T2 mapping sequence (E) and yellow-green in the T2 mapping sequence (C). MAGiC T1 mapping sequence (D) and MAGiC PD mapping sequence (F) show no abnormal pseudo-color display. SIJ, sacroiliac joint; T2WI FS, fat-suppressed T2 weighted imaging; T1WI, T1 weighted imaging; BME, bone marrow edema; MAGiC, magnetic resonance image compilation; PD, proton density.

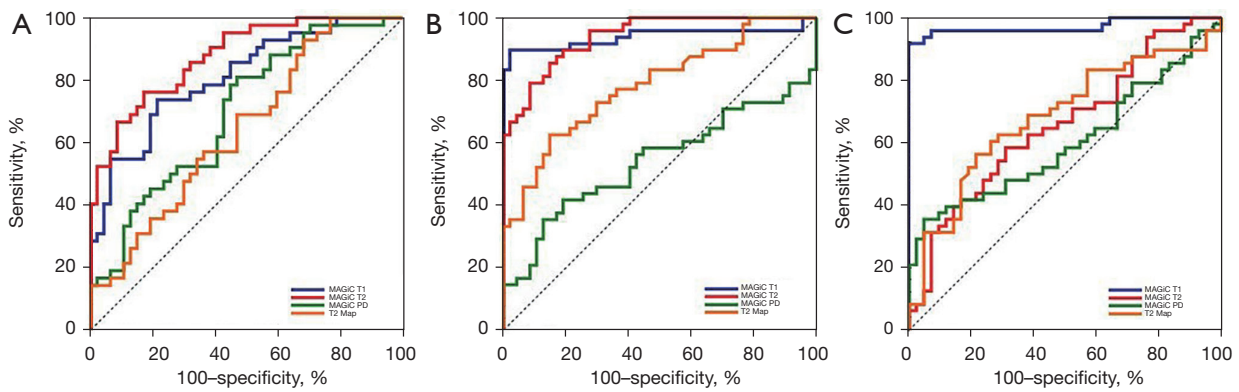

Figure 6 ROC curves of quantitative values (T1, T2, and PD values of the MAGiC sequence and T2 value of the T2 mapping sequence) among the three groups. (A) Comparisons of ROC curves of quantitative values for the inactive group and control group. The ROC curves demonstrate that MAGiC T1 and MAGiC T2 have a higher AUC, while T2 Map and MAGiC PD have a lower AUC. (B) Comparisons of ROC curves of quantitative values for the active group and control group. The ROC curves demonstrate that MAGiC T1 and MAGiC T2 have a higher AUC, followed by T2 Map, MAGiC PD has lowest AUC. (C) Comparisons of ROC curves of quantitative values for the inactive group and active group. The ROC curves demonstrate the MAGiC T1 has the highest AUC, followed by MAGiC T2 and T2 Map, MAGiC PD has the lowest AUC. MAGiC T1, T1 value of MAGiC sequence; MAGiC T2, T2 value of MAGiC sequence; MAGiC PD, PD value of MAGiC sequence; T2 map, T2 value of T2 mapping sequence; ROC, receiver operating characteristic; MAGiC, magnetic resonance image compilation; AUC, area under the curve; PD, proton density.

Table 5 Comparisons of ROC curves of quantitative values among the three groups

Variables	Inactive *vs.* control				Active *vs.* control				Inactive *vs.* active			
	MT1	MT2	MPD	TT2	MT1	MT2	MPD	TT2	MT1	MT2	MPD	TT2
Sensitivity (%)	73.81	76.19	80.95	92.86	89.58	79.17	35.42	62.50	91.67	58.33	35.42	56.25
Specificity (%)	78.72	82.98	53.19	31.91	97.87	91.49	87.23	85.11	100.00	69.05	95.24	78.57
PPV (%)	75.60	80.00	60.70	54.90	97.70	90.50	73.90	81.10	100.00	68.30	89.50	75.00
NPV (%)	77.10	79.60	75.80	83.30	90.20	81.10	56.90	69.00	91.30	59.20	56.30	61.10
AUC	0.812	0.877	0.698	0.644	0.938	0.940	0.540	0.784	0.971	0.655	0.600	0.681
Cutoff value	563.50	100.36	75.09	77.39	847.97	105.42	85.41	92.18	709.78	127.36	70.17	94.73
P value	MT1 *vs.* MT2: 0.1254; MT1 *vs.* TT2: 0.0106; MT2 *vs.* TT2: 0.0011				MT1 *vs.* MT2: 0.9724; MT1 *vs.* TT2: 0.0054; MT2 *vs.* TT2: 0.0021				MT1 *vs.* MT2: <0.0001; MT1 *vs.* TT2: <0.0001; MT2 *vs.* TT2: 0.7017			

ROC, receiver operating characteristic; MT1, T1 value of MAGiC sequence; MT2, T2 value of MAGiC sequence; MPD, PD value of MAGiC sequence; TT2, T2 value of T2 mapping sequence; PPV, positive predictive value; NPV, negative predictive value; AUC, area under the receiver operating characteristic curve; MAGiC, magnetic resonance image compilation; PD, proton density.

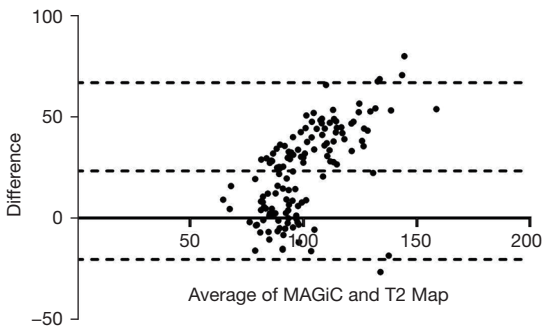

Figure 7 Bland-Altman plots for T2 values between MAGiC sequence and T2 mapping sequence. MAGiC, magnetic resonance image compilation.

and anisotropy of tissue matrix (22,23). It increases with tissue water content. Increases in the T1 value largely reflect the increase in free water content (24). As a result of inflammation of bone marrow, BME leads to osteopenia, vascular leakage, and increased local tissue water content, which give rise to the T1 value and T2 value (25,26). In MAGiC T1 mapping images, BME is displayed as red or yellow-green, and the corresponding BME areas in MAGiC T2 mapping images are displayed as yellow-green. A stronger signal intensity of BME indicates a more active degree of inflammation (27). The cutoff value of 709.78 ms was shown to differentiate active groups from inactive groups with high sensitivity (91.67%) and specificity (100%), which was higher than that of MAGiC T2 value (sensitivity: 58.33%, specificity: 69.05%). This renders the MAGiC T1 value a reliable quantitative parameter for diagnosing active sacroiliitis. If the value was greater than 709.78 ms, we considered this a case of active sacroiliitis, while a case of inactive sacroiliitis was defined as values less than 709.73 ms. *Table 5* shows the cut-off values for clinical reference, but a more extensive sample study is needed to verify our preliminary results.

Marty *et al.* (28) reported that the fat fraction in patients with Becker muscular dystrophy increased due to fat infiltration in the muscles, which made the average T1 values of thigh muscles significantly lower than those of healthy volunteers. Similarly, for patients with ax-SpA in the inactive stage, the partial BME decreased and lowered the water content in bone marrow. In contrast, the fat content increased, which resulted in lower MAGiC T1 and T2 values in the inactive group than in the active group, and a lower MAGiC T1 value in the inactive group than in the control group, but higher MAGiC T2 value in the inactive group than in the control group. Recent studies (29,30) have suggested that fat deposition under the articular surface in sacroiliitis is a prognostic factor in ax-SpA patients. Patients with fat deposition are more likely to develop structural damage, such as osseous fusion and ankylosing spondylitis. The results of this study reflected the pathophysiological changes of fat deposition for sacroiliitis in ax-SpA patients from the viewpoint of imaging. In addition, although the diagnostic efficiency of the MAGiC T1 value (cutoff value: 563.5 ms; sensitivity: 73.81%; specificity: 78.72%) was slightly lower than the MAGiC T2 value (cutoff value: 100.36 ms; sensitivity: 76.19%; specificity: 82.98%) in

the diagnosis of the inactive group and control group, the difference between the two groups was not statistically significant (P=0.1254). The MAGiC PD value differed between the inactive and control groups, but it offered little diagnostic value in general.

The MAGiC T1 value and the MAGiC T2 value in the active group and the inactive group were significantly higher than those in the control group, which means that these two parameters can possibly differentiate ax-SpA patients from healthy people, especially for ax-SpA patients without BME. In the future, we will include more patients and healthy volunteers to explore the feasibility of the diagnostic threshold of quantitative parameters to differentiate the two groups. Some patients with early-stage ax-SpA (stage I) may only present BME of sacroiliitis. Although some studies have reported that BME can also appear in some non-ax-SpA people, including runners, women with postpartum pain, and patients with condensing osteitis (31-34), all cases included in this study were older than 18 years and without a history of these diseases. Our results provide a potential method to help diagnose early-stage ax-SpA patients. However, more data need to be collected on early-stage ax-SpA patients and follow-up of these patients is required to confirm our findings.

Furthermore, by comparing the diagnostic performance of ROC curves, we also found that the MAGiC T2 value showed better diagnostic value than the T2 map T2 value. We speculated that this was related to the following aspects: on the one hand, the principles of the two sequences are different. The T2 mapping sequence is a multi-echo pulse sequence using fixed TR and TE to obtain different signal intensities at multiple TEs and calculate the T2 relaxation time of tissue, which can be described as 'imaging before calculation' (35). The MAGiC sequence can acquire T1, T2, PD, and radiofrequency field B1 values at one time based on the multi-dynamic, multi-echo (MDME) sequence to obtain the characteristic relaxation value of the tissue, which can be described as 'calculation before imaging'. Therefore, the MAGiC sequence can reflect signal changes of bone marrow more sensitively to yield a more accurate T2 value. Jiang *et al.* (15) proposed that the MAGiC T2 value of the lumbar intervertebral disc in people with low back pain was highly positively correlated with the T2 map T2 value (r=0.962; P<0.01), which was inconsistent with the result of our study. We hypothesized that the mechanism of intervertebral disc degeneration is the loss of intervertebral disc water content and proteoglycan, which leads to the decrease of T2 value (36). The structures of SIJ are relatively complex, and many kinds of lesions can occur in subchondral areas. The measurement of the T2 mapping sequence is susceptible to influence by surrounding tissues, which may result in unstable measurement values. On the other hand, the measurement values of the MAGiC sequence and T2 mapping sequence in this study were based on manually delineating the ROI. Although the inter- and intra-reader agreement of the two sequences was good, the possible measurement differences still cannot be avoided.

Our study had some limitations. First, with the increase of age, the proportion of yellow bone marrow increases (37). Therefore, further research should compare the quantitative value of the MAGiC sequence by age groups. Second, a previous study found that T2 map T2 values vary for different sequences and parameters (38). As a quantitative technique, the influence of different parameter settings on the MAGiC sequence is not yet known. Third, our research was mainly based on MRI images; we have not yet explored the correlation between quantitative values and clinical indicators and their significance in evaluating the efficacy of ax-SpA patients. Fourth, in view of the overall scanning time of patients, this study failed to compare the difference between the conventional T1 mapping sequence and the MAGiC T1 mapping sequence, which needs to be further explored.

In conclusion, our findings show that the MAGiC sequence, as a new MRI method, can directly quantify active sacroiliitis. The MAGiC T1 value and T2 value have diagnostic value for active sacroiliitis in patients with ax-SpA; the MAGiC T1 diagnostic value is higher than that of MAGiC T2, while the MAGiC PD value has limited diagnostic value. The efficacy of the MAGiC T2 value was higher than that of the T2 map T2 value.

Acknowledgments

Funding: This study was supported by the Guangdong Basic and Applied Basic Research Foundation, China (No. 2019A1515010818 and No. 2020A1515010395), the Science and Technology Project in the Social Development Field of Zhuhai City, Guangdong Province, China (No. ZH22036201210066PWC) and the Clinical IIT Research Project of the Fifth Affiliated Hospital of Sun Yat-sen University (No. YNZZ2020-06).

Footnote

Reporting Checklist: The authors have completed the STARD

reporting checklist. Available at https://qims.amegroups.com/article/view/10.21037/qims-21-972/rc

Conflicts of Interest: All authors have completed the ICMJE uniform disclosure form (available at https://qims.amegroups.com/article/view/10.21037/qims-21-972/coif). The authors have no conflicts of interest to declare.

Ethical Statement: The authors are accountable for all aspects of the work in ensuring that questions related to the accuracy or integrity of any part of the work are appropriately investigated and resolved. The study was conducted in accordance with the Declaration of Helsinki (as revised in 2013). The study was approved by the Ethics Committee of the Fifth Affiliated Hospital of Sun Yat-sen University [No. K160-1(2019)], and informed consent was provided by all individual participants.

References

1. Sieper J, Poddubnyy D. Axial spondyloarthritis. Lancet 2017;390:73-84.
2. Sieper J, Rudwaleit M, Baraliakos X, Brandt J, Braun J, Burgos-Vargas R, Dougados M, Hermann KG, Landewé R, Maksymowych W, van der Heijde D. The Assessment of SpondyloArthritis international Society (ASAS) handbook: a guide to assess spondyloarthritis. Ann Rheum Dis 2009;68 Suppl 2:ii1-44.
3. Maksymowych WP, Chiowchanwisawakit P, Clare T, Pedersen SJ, Østergaard M, Lambert RG. Inflammatory lesions of the spine on magnetic resonance imaging predict the development of new syndesmophytes in ankylosing spondylitis: evidence of a relationship between inflammation and new bone formation. Arthritis Rheum 2009;60:93-102.
4. Bollow M, Fischer T, Reisshauer H, Backhaus M, Sieper J, Hamm B, Braun J. Quantitative analyses of sacroiliac biopsies in spondyloarthropathies: T cells and macrophages predominate in early and active sacroiliitis-cellularity correlates with the degree of enhancement detected by magnetic resonance imaging. Ann Rheum Dis 2000;59:135-40.
5. Bane O, Wagner M, Zhang JL, Dyvorne HA, Orton M, Rusinek H, Taouli B. Assessment of renal function using intravoxel incoherent motion diffusion-weighted imaging and dynamic contrast-enhanced MRI. J Magn Reson Imaging 2016;44:317-26.
6. Bae KT. Peak contrast enhancement in CT and MR angiography: when does it occur and why? Pharmacokinetic study in a porcine model. Radiology 2003;227:809-16.
7. Bradbury LA, Hollis KA, Gautier B, Shankaranarayana S, Robinson PC, Saad N, Lê Cao KA, Brown MA. Diffusion-weighted Imaging Is a Sensitive and Specific Magnetic Resonance Sequence in the Diagnosis of Ankylosing Spondylitis. J Rheumatol 2018;45:771-8.
8. Beltran LS, Samim M, Gyftopoulos S, Bruno MT, Petchprapa CN. Does the Addition of DWI to Fluid-Sensitive Conventional MRI of the Sacroiliac Joints Improve the Diagnosis of Sacroiliitis? AJR Am J Roentgenol 2018;210:1309-16.
9. Le Bihan D, Breton E, Lallemand D, Grenier P, Cabanis E, Laval-Jeantet M. MR imaging of intravoxel incoherent motions: application to diffusion and perfusion in neurologic disorders. Radiology 1986;161:401-7.
10. Zhao YH, Li SL, Liu ZY, Chen X, Zhao XC, Hu SY, Liu ZH, M S YJ, Chan Q, Liang CH. Detection of Active Sacroiliitis with Ankylosing Spondylitis through Intravoxel Incoherent Motion Diffusion-Weighted MR Imaging. Eur Radiol 2015;25:2754-63.
11. Wang D, Yin H, Liu W, Li Z, Ren J, Wang K, Han D. Comparative analysis of the diagnostic values of T2 mapping and diffusion-weighted imaging for sacroiliitis in ankylosing spondylitis. Skeletal Radiol 2020;49:1597-606.
12. Albano D, Bignone R, Chianca V, Cuocolo R, Messina C, Sconfienza LM, Ciccia F, Brunetti A, Midiri M, Galia M. T2 mapping of the sacroiliac joints in patients with axial spondyloarthritis. Eur J Radiol 2020;131:109246.
13. Fernquest S, Palmer A, Gammer B, Hirons E, Kendrick B, Taylor A, De Berker H, Bangerter N, Carr A, Glyn-Jones S. Compositional MRI of the Hip: Reproducibility, Effect of Joint Unloading, and Comparison of T2 Relaxometry with Delayed Gadolinium-Enhanced Magnetic Resonance Imaging of Cartilage. Cartilage 2021;12:418-30.
14. Warntjes JB, Leinhard OD, West J, Lundberg P. Rapid magnetic resonance quantification on the brain:

Optimization for clinical usage. Magn Reson Med 2008;60:320-9.
15. Jiang Y, Yu L, Luo X, Lin Y, He B, Wu B, Qu J, Wu T, Pu-Yeh W, Zhang C, Li C, Chen M. Quantitative synthetic MRI for evaluation of the lumbar intervertebral disk degeneration in patients with chronic low back pain. Eur J Radiol 2020;124:108858.
16. Lee SH, Lee YH, Hahn S, Yang J, Song HT, Suh JS. Optimization of T2-weighted imaging for shoulder magnetic resonance arthrography by synthetic magnetic resonance imaging. Acta Radiol 2018;59:959-65.
17. Kumar NM, Fritz B, Stern SE, Warntjes JBM, Lisa Chuah YM, Fritz J. Synthetic MRI of the Knee: Phantom Validation and Comparison with Conventional MRI. Radiology 2018;289:465-77.
18. Roux M, Hilbert T, Hussami M, Becce F, Kober T, Omoumi P. MRI T2 Mapping of the Knee Providing Synthetic Morphologic Images: Comparison to Conventional Turbo Spin-Echo MRI. Radiology 2019;293:620-30.
19. Proft F, Poddubnyy D. Ankylosing spondylitis and axial spondyloarthritis: recent insights and impact of new classification criteria. Ther Adv Musculoskelet Dis 2018;10:129-39.
20. Maksymowych WP, Inman RD, Salonen D, Dhillon SS, Williams M, Stone M, Conner-Spady B, Palsat J, Lambert RG. Spondyloarthritis research Consortium of Canada magnetic resonance imaging index for assessment of sacroiliac joint inflammation in ankylosing spondylitis. Arthritis Rheum 2005;53:703-9.
21. Maksymowych WP, Lambert RG, Østergaard M, Pedersen SJ, Machado PM, Weber U, et al. MRI lesions in the sacroiliac joints of patients with spondyloarthritis: an update of definitions and validation by the ASAS MRI working group. Ann Rheum Dis 2019;78:1550-8.
22. Harrison R, Bronskill MJ, Henkelman RM. Magnetization transfer and T2 relaxation components in tissue. Magn Reson Med 1995;33:490-6.
23. Packer KJ. The dynamics of water in heterogeneous systems. Philos Trans R Soc Lond B Biol Sci 1977;278:59-87.
24. Williams ES, Kaplan JI, Thatcher F, Zimmerman G, Knoebel SB. Prolongation of proton spin lattice relaxation times in regionally ischemic tissue from dog hearts. J Nucl Med 1980;21:449-53.
25. Dalbeth N, Smith T, Gray S, Doyle A, Antill P, Lobo M, Robinson E, King A, Cornish J, Shalley G, Gao A, McQueen FM. Cellular haracterization of magnetic resonance imaging bone oedema in rheumatoid arthritis; implications for pathogenesis of erosive disease. Ann Rheum Dis 2009;68:279-82.
26. Watad A, Bridgewood C, Russell T, Marzo-Ortega H, Cuthbert R, McGonagle D. The Early Phases of Ankylosing Spondylitis: Emerging Insights From Clinical and Basic Science. Front Immunol 2018;9:2668.
27. Lambert RG, Bakker PA, van der Heijde D, Weber U, Rudwaleit M, Hermann KG, et al. Defining active sacroiliitis on MRI for classification of axial spondyloarthritis: update by the ASAS MRI working group. Ann Rheum Dis 2016;75:1958-63.
28. Marty B, Coppa B, Carlier PG. Monitoring skeletal muscle chronic fatty degenerations with fast T1-mapping. Eur Radiol 2018;28:4662-8.
29. Kang KY, Kim IJ, Yoon MA, Hong YS, Park SH, Ju JH. Fat Metaplasia on Sacroiliac Joint Magnetic Resonance Imaging at Baseline Is Associated with Spinal Radiographic Progression in Patients with Axial Spondyloarthritis. PloS One 2015;10:e0135206.
30. Maksymowych WP. Imaging in Axial Spondyloarthritis: Evaluation of Inflammatory and Structural Changes. Rheum Dis Clin North Am 2016;42:645-62.
31. Weber U, Jurik AG, Zejden A, Larsen E, Jørgensen SH, Rufibach K, Schioldan C, Schmidt-Olsen S. Frequency and Anatomic Distribution of Magnetic Resonance Imaging Features in the Sacroiliac Joints of Young Athletes: Exploring "Background Noise" Toward a Data-Driven Definition of Sacroiliitis in Early Spondyloarthritis. Arthritis Rheumatol 2018;70:736-45.
32. de Winter J, de Hooge M, van de Sande M, de Jong H, van Hoeven L, de Koning A, Berg IJ, Ramonda R, Baeten D, van der Heijde D, Weel A, Landewé R. Magnetic Resonance Imaging of the Sacroiliac Joints Indicating Sacroiliitis According to the Assessment of SpondyloArthritis international Society Definition in Healthy Individuals, Runners, and Women With Postpartum Back Pain. Arthritis Rheumatol 2018;70:1042-8.
33. Eshed I, Miloh-Raz H, Dulitzki M, Lidar Z, Aharoni D, Liberman B, Lidar M. Peripartum changes of the sacroiliac joints on MRI: increasing mechanical load correlating with signs of edema and inflammation kindling spondyloarthropathy in the genetically prone. Clin Rheumatol 2015;34:1419-26.
34. Ma L, Gao Z, Zhong Y, Meng Q. Osteitis condensans

ilii may demonstrate bone marrow edema on sacroiliac joint magnetic resonance imaging. Int J Rheum Dis 2018;21:299-307.
35. Mosher TJ, Dardzinski BJ. Cartilage MRI T2 relaxation time mapping: overview and applications. Semin Musculoskelet Radiol 2004;8:355-68.
36. Modic MT, Ross JS. Lumbar degenerative disk disease. Radiology 2007;245:43-61.
37. Dawson KL, Moore SG, Rowland JM. Age-related marrow changes in the pelvis: MR and anatomic findings. Radiology 1992;183:47-51.
38. Pai A, Li X, Majumdar S. A comparative study at 3 T of sequence dependence of T2 quantitation in the knee. Magn Reson Imaging 2008;26:1215-20.

Cite this article as: Jiang Y, Li W, Zheng J, Zhang K, Liu C, Hong G. Magnetic resonance image compilation sequence to quantitatively detect active sacroiliitis with axial spondyloarthritis. Quant Imaging Med Surg 2022;12(7):3666-3678. doi: 10.21037/qims-21-972

